Journal of
Applied Remote Sensing

RemoteSensing.SPIEDigitalLibrary.org

Crop classification from Sentinel-2-derived vegetation indices using ensemble learning

Rei Sonobe
Yuki Yamaya
Hiroshi Tani
Xiufeng Wang
Nobuyuki Kobayashi
Kan-ichiro Mochizuki

SPIE.

Rei Sonobe, Yuki Yamaya, Hiroshi Tani, Xiufeng Wang, Nobuyuki Kobayashi, Kan-ichiro Mochizuki, "Crop classification from Sentinel-2-derived vegetation indices using ensemble learning," *J. Appl. Remote Sens.* **12**(2), 026019 (2018), doi: 10.1117/1.JRS.12.026019.

Crop classification from Sentinel-2-derived vegetation indices using ensemble learning

Rei Sonobe,[a,*] Yuki Yamaya,[b] Hiroshi Tani,[c] Xiufeng Wang,[c] Nobuyuki Kobayashi,[d] and Kan-ichiro Mochizuki[e]

[a]Shizuoka University, Faculty of Agriculture, Shizuoka, Japan
[b]Hokkaido University, Graduate School of Agriculture, Sapporo, Japan
[c]Hokkaido University, Research Faculty of Agriculture, Sapporo, Japan
[d]Smart Link Hokkaido, Iwamizawa, Japan
[e]PASCO Corporation, Tokyo, Japan

Abstract. The identification and mapping of crops are important for estimating potential harvest as well as for agricultural field management. Optical remote sensing is one of the most attractive options because it offers vegetation indices and some data have been distributed free of charge. Especially, Sentinel-2A, which is equipped with a multispectral sensor (MSI) with blue, green, red, and near-infrared-1 bands at 10 m; red edge 1 to 3, near-infrared-2, and shortwave infrared 1 and 2 at 20 m; and 3 atmospheric bands (band 1, band 9, and band 10) at 60 m, offer some vegetation indices calculated to assess vegetation status. However, sufficient consideration has not been given to the potential of vegetation indices calculated from MSI data. Thus, 82 published indices were calculated and their importance were evaluated for classifying crop types. The two most common classification algorithms, random forests (RF) and support vector machine (SVM), were applied to conduct cropland classification from MSI data. Additionally, super learning was applied for more improvement, achieving overall accuracies of 90.2% to 92.2%. Of the two algorithms applied (RF and SVM), the accuracy of SVM was superior and 89.3% to 92.0% of overall accuracies were confirmed. Furthermore, stacking contributed to higher overall accuracies (90.2% to 92.2%), and significant differences were confirmed with the results of SVM and RF. Our results showed that vegetation indices had the greatest contributions in identifying specific crop types. [DOI: 10.1117/1.JRS.12.026019]

Keywords: crop; random forests; Sentinel-2; stacking; support vector machine; vegetation index.

Paper 180133 received Feb. 12, 2018; accepted for publication May 7, 2018; published online May 18, 2018.

1 Introduction

From a land-planning perspective, cropland diversity is vital and crop cover maps provide information for estimating potential harvest and agricultural field management. To document field properties, such as cultivated crops and locations, some local governments in Japan have been using manual methods.[1] However, more efficient techniques are required to reduce the high expense of these methods. Thus, satellite data-based cropland mapping has gained attention. Some spectral indices, which are combinations of spectral measurements at different wavelengths, have been used to evaluate phenology or quantify biophysical parameters.[2–5] As a result, they have also made crop maps more accurate in previous studies,[6] and the abilities of optical remote sensing data have been improved for monitoring agricultural fields. The opportunities to obtain optical remote sensing data have improved due to the Sentinel-2A satellite launch on June 23, 2015. Now, it is collecting multispectral data including 13 bands covering the visible, shortwave infrared bands (SWIR) wavelength regions. Sentinel-2B, which possesses the same

*Address all correspondence to: Rei Sonobe, E-mail: reysnb@gmail.com

1931-3195/2018/$25.00 © 2018 SPIE

specifications, was launched on March 7, 2017, and creates greater opportunities for monitoring agricultural fields. Furthermore, various spectral indices can be extracted including indices based on SWIR, which are influenced by plant constituents, such as pigments, leaf water contents, and biochemicals.[7,8] Furthermore, vegetation indices derived from reflectance data acquired from optical sensors have been widely used to assess variations in the physiological states and biophysical properties of vegetation.[9–11] Specifically, the normalized difference vegetation index (NDVI),[12] soil-adjusted vegetation index (SAVI),[13] and enhanced vegetation index (EVI)[14] have been used for monitoring vegetation systems or ecological responses to environmental change.[15] Multispectral sensor (MSI) data have been used for identifying crop types,[16–18] plastic-covered greenhouses,[19] water bodies,[20] and some previous studies showed the potential of VIs calculated from MSI data. However, it is possible to calculate a vast number of VIs from MSI data and most of them have been ignored in the previous studies. In this study, 82 published indices and original reflectance data sources were evaluated to classify six crop types including beans, beetroot, grass, maize, potato, and winter wheat, which are dominant crops on the western Tokachi plain, Hokkaido, Japan.

In addition to qualities of remote sensing data, classification algorithms are important to improve classification accuracies of crop maps. Recently, random forests (RF) is a widely used machine learning algorithm consisting of an ensemble of decision trees, and it has been an extremely successful machine learning algorithm for classification and regression method.[21] It has been applied for generating land cover maps[22,23] and reached around 65% (tree species identification),[17] 76% (crop types identification),[17] and 90% (greenhouse detection)[19] using MSI data in the previous studies.

Some studies showed that support vector machine (SVM) performed better than RF for this purpose, and it has been widely applied for crop-for-crop classification.[22,24–26] Its robustness to outliers has been demonstrated and SVM is an excellent classifier when the number of input features is large.[27]

The superlearner (SL) methodology,[25] also called stacking, is an ensemble learning method in which the user-supplied library of algorithms is combined through a convex weighted combination, with the optimal weights to make the cross-validated empirical risk smaller. Therefore, SL could be expected to classify crop types more accurately than the single use of RF or SVM, both considered in this study. Next, an ensemble approach based on SL was applied for improving classification accuracies.

Within this framework, the main objectives of the present study were to evaluate the potential of Sentinel-2 data for crop-type classification and the potential of ensemble learning based on RF and SVM.

2 Materials and Methods

2.1 *Study Area*

The study area was located in the western part of Tokachi plain, Hokkaido, Japan (Fig. 1, 142°42′51″ to 143°08′47″ E, 42°43′20″ to 43°07′24″ N). Main cultivated crop types are beans, beetroots, grasses, maize, potatoes, and winter wheat. The average monthly temperatures were 8.3°C to 21.8°C and monthly precipitation was 12.0 to 94.5 mm from May to October.

Field location and attribute data, such as crop types, were based on manual surveys and provided by Tokachi Nosai (Obihiro, Hokkaido) as a polygon-shaped file. A total of 12,639 fields [2265 beans fields, 1548 beetroot fields, 2110 grasslands (timothy and orchard grass), 1000 maize fields, 2452 potato fields, and 3264 winter wheat fields] were observed. The fields ranged from 0.05 to 18.21 ha with an averaged value of 2.54 ha. Grasslands were located on the outskirts of the built-up area.

2.2 *Remote Sensing Data*

The data acquired from Sentinel-2 MSI contained blue, green, red, and near-infrared-1 bands at 10 m; red edge 1 to 3, near-infrared-2, and SWIR 1 and 2 at 20 m; and three atmospheric bands

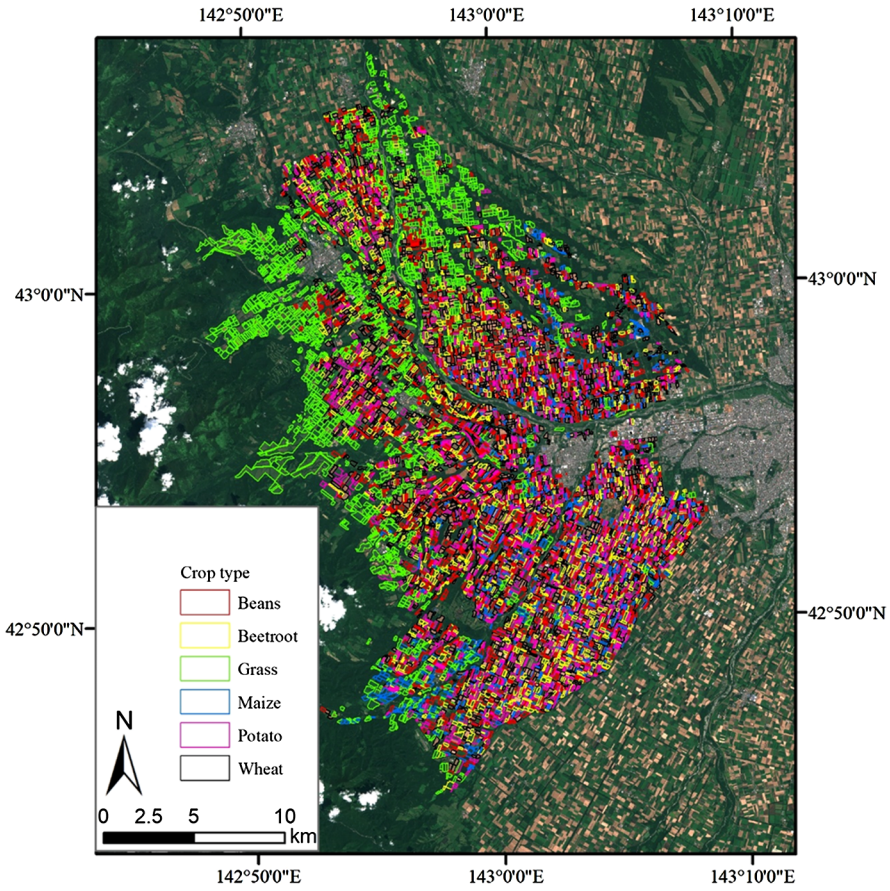

Fig. 1 Study area and the distribution of croplands (background map shows Sentinel-2A data obtained on August 11, 2016, R: band 4, G: band 3, and B: band 2).

(band 1, band 9, and band 10) at 60 m. In this study, the three atmospheric bands were removed, because they were dedicated to atmospheric corrections and cloud screening.[28]

Although Sentinel-2A imagery was gathered seven times from May to September 2016, for the whole site, all images were covered with clouds except for one acquired on 11 August. The level 1C data acquired on August 11, 2016, were downloaded from EarthExplorer.[29] All bands were converted to 10-m resolution with a cubic convolution resampling method and average reflectance values of each band were calculated for each field using the field polygons to compensate for spatial variability and to avoid problems related to uncertainty in georeferencing.

Some vegetation indices, such as NDVI, have been used for improving classification accuracies in previous studies.[16,22,30,31] About 82 published vegetation indices for evaluating various vegetation properties were calculated in this study (Table 1).

2.3 *Classification Algorithm*

All samples were divided into the following three groups using a stratified random sampling approach: training data (50%) for developing classification models, validation data (25%) for hyperparameter tuning, and test data (25%) for evaluation of classification accuracies[86] and Table 2 shows the numbers of fields of each crop type.

SVM partitions data using maximum separation margins[87] and the "kernel trick" has frequently been applied instead of attempting to fit a nonlinear model in previous studies.[30] In this study, the Gaussian radial basis function kernel, which has mostly been used for classification purposes,[30] was used as a kernel and two parameters were tuned to control the flexibility of the classifier, the regularization parameter C, and the kernel bandwidth γ. If the C value is too large, there is a high penalty for no separable points, and we may store many support vectors and

Table 1 Vegetation indices calculated from Sentinel-2 MSI data.

Abbreviation	Index	Formula
AFRI1.6[32]	Aerosol free vegetation index 1.6	$\frac{\text{Band8}a-0.66*\text{Band11}}{\text{Band8}a+0.66*\text{Band11}}$
AFRI2.1[32]	Aerosol free vegetation index 2.1	$\frac{\text{Band8}a-0.5*\text{Band12}}{\text{Band8}a+0.5*\text{Band12}}$
ARI[33]	Anthocyanin reflectance index	$\frac{1}{\text{Band3}}-\frac{1}{\text{Band5}}$
ARVI[34]	Atmospherically resistant vegetation index	$\frac{\{\text{Band8}-[\text{Band4}-\gamma(\text{Band2}-\text{Band4})]\}}{\{\text{Band8}+[\text{Band4}-\gamma(\text{Band2}-\text{Band4})]\}}$ The γ is a weighting function that depends on aerosol type. In this study, a value of 1 for γ.
ARVI2[34]	Atmospherically resistant vegetation index 2	$-0.18+1.17*\left(\frac{\text{Band8}-\text{Band4}}{\text{Band8}+\text{Band4}}\right)$
ATSAVI[35]	Adjusted transformed soil-adjusted vegetation index	$\frac{a*(\text{Band8}-a*\text{Band4}-b)}{\text{Band8}+\text{Band4}-ab+X(1+a^2)}$ $a=1.22,\ b=0.03,\ X=0.08$
AVI[36]	Ashburn vegetation index	$2*\text{Band8}a-\text{Band4}$
BNDVI[37]	Blue-normalized difference vegetation index	$(\text{Band8}-\text{Band2})/(\text{Band8}+\text{Band2})$
BRI[38]	Browning reflectance index	$\frac{1/\text{Band3}-1/\text{Band5}}{\text{Band6}}$
BWDRVI[39]	Blue-wide dynamic range vegetation index	$\frac{0.1*\text{Band7}-\text{Band2}}{0.1*\text{Band7}+\text{Band2}}$
CARI[40]	Chlorophyll absorption ratio index	$\frac{\text{Band5}*\sqrt{(a*\text{Band4}+\text{Band4}+b)^2}}{\text{Band4}}*(a^2+1)^{0.5}$ $a=(\text{Band5}-\text{Band3})/150$ $b=\text{Band3}*550*a$
CCCI[41]	Canopy chlorophyll content index	$\frac{\left(\frac{\text{Band8}-\text{Band5}}{\text{Band8}+\text{Band5}}\right)}{\left(\frac{\text{Band8}-\text{Band4}}{\text{Band8}+\text{Band4}}\right)}$
CRI550[42]	Carotenoid reflectance index 550	$\frac{1}{\text{Band2}}-\frac{1}{\text{Band3}}$
CRI700[42]	Carotenoid reflectance index 700	$\frac{1}{\text{Band2}}-\frac{1}{\text{Band5}}$
CVI[43]	Chlorophyll vegetation index	$\frac{\text{Band8}*\text{Band4}}{(\text{Band3})^2}$
Datt1[44]	Vegetation index proposed by Datt 1	$\frac{\text{Band8}-\text{Band5}}{\text{Band8}-\text{Band4}}$
Datt2[45]	Vegetation index proposed by Datt 2	$\frac{\text{Band4}}{\text{Band3}*\text{Band5}}$
Datt3[45]	Vegetation index proposed by Datt 3	$\frac{\text{Band8a}}{\text{Band3}*\text{Band5}}$
DVI[46]	Differenced vegetation index	$2.4*\text{Band8}-\text{Band4}$
EPIcar[45]	Eucalyptus pigment index for carotenoid	$0.0049*\left(\frac{\text{Band4}}{\text{Band3}*\text{Band5}}\right)^{0.7488}$
EPIChla[45]	Eucalyptus pigment index for chlorophyll a	$0.0161*\left(\frac{\text{Band4}}{\text{Band3}*\text{Band5}}\right)^{0.7784}$
EPIChlab[45]	Eucalyptus pigment index for chlorophyll a+b	$0.0236*\left(\frac{\text{Band4}}{\text{Band3}*\text{Band5}}\right)^{0.7954}$
EPIChlb[45]	Eucalyptus pigment index for chlorophyll b	$0.0337*\left(\frac{\text{Band4}}{\text{Band3}}\right)^{1.8695}$
EVI[14]	Enhanced vegetation index	$2.5*\frac{\text{Band8}-\text{Band4}}{\text{Band8}+6*\text{Band4}-7.5*\text{Band2}+1}$
EVI2[47]	Enhanced vegetation index 2	$2.4*\frac{\text{Band8}-\text{Band4}}{\text{Band8}+\text{Band4}+1}$
EVI2.2[48]	Enhanced vegetation index 2.2	$2.5*\frac{\text{Band8}-\text{Band4}}{\text{Band8}+2.4*\text{Band4}+1}$

Table 1 (*Continued*).

Abbreviation	Index	Formula
GARI[49]	Green atmospherically resistant vegetation index	$\frac{\text{Band8}-[\text{Band3}-(\text{Band2}-\text{Band4})]}{\text{Band8}-[\text{Band3}+(\text{Band2}-\text{Band4})]}$
GBNDVI[50]	Green-Blue normalized difference vegetation index	$\frac{\text{Band8}-(\text{Band3}+\text{Band2})}{\text{Band8}+(\text{Band3}+\text{Band2})}$
GDVI[51]	Green difference vegetation index	$\text{Band8} - \text{Band3}$
GEMI[52]	Global environment monitoring index	$\frac{n*(1-0.25*n)-\text{Band4}-0.125}{1-\text{Band4}}$ $n = \frac{2*\text{Band5}^2-\text{Band4}^2+1.5*\text{Band5}+0.5*\text{Band4}}{\text{Band5}+\text{Band4}+0.5}$
GLI[53]	Green leaf index	$\frac{2*\text{Band3}-\text{Band5}-\text{Band2}}{2*\text{Band3}+\text{Band5}+\text{Band2}}$
GNDVI[49]	Green normalized difference vegetation index	$\frac{\text{Band8}-\text{Band3}}{\text{Band8}+\text{Band3}}$
GNDVI2[49]	Green normalized difference vegetation index 2	$\frac{\text{Band7}-\text{Band3}}{\text{Band7}+\text{Band3}}$
GOSAVI[54]	Green optimized soil-adjusted vegetation index	$\frac{\text{Band8}-\text{Band3}}{\text{Band8}+\text{Band3}+0.16}$
GRNDVI[55]	Green–red normalized difference vegetation index	$\frac{\text{Band8}-(\text{Band3}+\text{Band5})}{\text{Band8}+(\text{Band3}+\text{Band5})}$
GVMI[56]	Global vegetation moisture index	$\frac{(\text{Band8}+0.1)-(\text{Band12}+0.02)}{(\text{Band8}+0.1)+(\text{Band12}+0.02)}$
Hue[57]	Hue	$a\tan\left[\frac{2*\text{Band5}-\text{Band3}-\text{Band2}}{30.5} * (\text{Band3} - \text{Band2})\right]$
IPVI[58]	Infrared percentage vegetation index	$\frac{\frac{\text{Band8}}{\text{Band8}+\text{Band5}}}{2}\left(\frac{\text{Band5}-\text{Band3}}{\text{Band5}+\text{Band5}}+1\right)$
LCI[44]	Leaf chlorophyll index	$\frac{\text{Band8}-\text{Band5}}{\text{Band8}+\text{Band4}}$
Maccion[59]	Vegetation index proposed by Maccioni	$\frac{\text{Band7}-\text{Band5}}{\text{Band7}-\text{Band4}}$
MCARI[60]	Modified chlorophyll absorption in reflectance index	$[(\text{Band5} - \text{Band4}) - 0.2 * (\text{Band5} - \text{Band3})] * \frac{\text{Band5}}{\text{Band4}}$
MCARI/MTVI2[61]	MCARI/MTVI2	MCARI/MTVI2
MCARI/OSAVI[62]	MCARI/OSAVI	MCARI/OSAVI
MCARI1[62]	Modified chlorophyll absorption in reflectance index 1	$1.2 * [2.5 * (\text{Band8} - \text{Band4}) - 1.3 * (\text{Band8} - \text{Band3})]$
MCARI2[62]	Modified chlorophyll absorption in reflectance index 2	$1.5 * \frac{2.5*(\text{Band8}-\text{Band4})-1.3*(\text{Band8}-\text{Band3})}{\sqrt{(2*\text{Bamd8}+1)^2-(6*\text{Band8}-5*\sqrt{\text{Band4}})-0.5}}$
MGVI[63]	Green vegetation index proposed by Misra	$-0.386 * \text{Band3} - 0.530 * \text{Band4} + 0.535 * \text{Band6} + 0.532 * \text{Band8}$
mNDVI[64]	Modified normalized difference vegetation index	$\frac{\text{Band8}-\text{Band4}}{\text{Band8}+\text{Band4}-2*\text{Band2}}$
MNSI[63]	Non such index proposed by Misra	$0.404 * \text{Band3} + 0.039 * \text{Band4} - 0.505 * \text{Band6} + 0.762 * \text{Band8}$
MSAVI[65]	Modified soil-adjusted vegetation index	$\frac{2*\text{Band8}+1-\sqrt{(2*\text{Band8}+1)^2-8*(\text{Band8}-\text{Band5})}}{2}$
MSAVI2[65]	Modified soil-adjusted vegetation index 2	$\frac{2*\text{Band8}+1-\sqrt{(2*\text{Band8}+1)^2-8*(\text{Band8}-\text{Band4})}}{2}$
MSBI[63]	Soil brightness index proposed by Misra	$0.406 * \text{Band3} + 0.600 * \text{Band4} + 0.645 * \text{Band6} + 0.243 * \text{Band8}$

Table 1 (*Continued*).

Abbreviation	Index	Formula
MSR670[66]	Modified simple ratio 670/800	$\frac{\frac{\text{Band8}}{\text{Band4}}-1}{\sqrt{\frac{\text{Band8}}{\text{Band4}}+1}}$
MSRNir/Red[67]	Modified simple ratio NIR/red	$\frac{\frac{\text{Band8}}{\text{Band5}}-1}{\sqrt{\frac{\text{Band8}}{\text{Band5}}+1}}$
MTVI2[62]	Modified triangular vegetation index 2	$1.5*\frac{1.2*(\text{Band8}-\text{Band3})-2.5*(\text{Band4}-\text{Band3})}{\sqrt{(2*\text{Bamd8}+1)^2-(6*\text{Band8}-5*\sqrt{\text{Band4}})-0.5}}$
NBR[68]	Normalized difference NIR/SWIR normalized burn ratio	$\frac{\text{Band8}-\text{Band12}}{\text{Band8}+\text{Band12}}$
ND774/677[69]	Normalized difference 774/677	$\frac{\text{Band7}-\text{Band4}}{\text{Band7}+\text{Band4}}$
NDII[70]	Normalized difference infrared index	$\frac{\text{Band8}-\text{Band11}}{\text{Band8}+\text{Band11}}$
NDRE[71]	Nnormalized difference red-edge	$\frac{\text{Band7}-\text{Band5}}{\text{Band7}+\text{Band5}}$
NDSI[72]	Normalized difference salinity index	$\frac{\text{Band11}-\text{Band12}}{\text{Band11}+\text{Band12}}$
NDVI[12]	Normalized difference vegetation index	$\frac{\text{Band8}-\text{Band4}}{\text{Band8}+\text{Band4}}$
NDVI2[51]	Normalized difference vegetation index 2	$\frac{\text{Band12}-\text{Band8}}{\text{Band12}+\text{Band8}}$
NGRDI[69]	Normalized green red difference index	$\frac{\text{Band3}-\text{Band5}}{\text{Band3}+\text{Band5}}$
OSAVI[54,73]	Optimized soil-adjusted vegetation index	$1.16*\frac{\text{Band8}-\text{Band4}}{\text{Band8}+\text{Band4}+0.16}$
PNDVI[55]	Pan normalized difference vegetation index	$\frac{\text{Band8}-(\text{Band3}+\text{Band5}+\text{Band2})}{\text{Band8}+(\text{Band3}+\text{Band5}+\text{Band2})}$
PVR[74]	Photosynthetic vigor ratio	$\frac{\text{Band3}-\text{Band4}}{\text{Band3}+\text{Band4}}$
RBNDVI[55]	Red–blue normalized difference vegetation index	$\frac{\text{Band8}-(\text{Band4}+\text{Band2})}{\text{Band8}+(\text{Band4}+\text{Band2})}$
RDVI[75]	Renormalized difference vegetation index	$\frac{\text{Band8}-\text{Band4}}{\sqrt{\text{Band8}+\text{Band4}}}$
REIP[76]	Red-edge inflection point	$700+40*\left[\frac{\left(\frac{\text{Band4}+\text{Band7}}{2}\right)-\text{Band5}}{\text{Band6}-\text{Band5}}\right]$
Rre[77]	Reflectance at the inflexion point	$\frac{\text{Band4}+\text{Band7}}{2}$
SAVI[13]	Soil adjusted vegetation index	$1.5*\frac{\text{Band8}-\text{Band4}}{\text{Band8}+\text{Band4}+0.5}$
SBL[46]	Soil background line	$\text{Band8}-2.4*\text{Band4}$
SIPI[78]	Structure intensive pigment index	$\frac{\text{Band8}-\text{Band2}}{\text{Band8}-\text{Band4}}$
SIWSI[79]	Shortwave infrared water stress index	$\frac{\text{Band8}a-\text{Band11}}{\text{Band8}a+\text{Band11}}$
SLAVI[80]	Specific leaf area vegetation index	$\frac{\text{Band8}}{\text{Band4}+\text{Band12}}$
TCARI[60]	Transformed chlorophyll absorption ratio	$3*\left[(\text{Band5}-\text{Band4})-0.2*(\text{Band5}-\text{Band3})\left(\frac{\text{Band5}}{\text{Band4}}\right)\right]$
TCARI/OSAVI[73]	TCARI/OSAVI	TCARI/OSAVI
TCI[43,81]	Triangular chlorophyll index	$1.2*(\text{Band5}-\text{Band3})-1.5*(\text{Band4}-\text{Band3})*\sqrt{\frac{\text{Band5}}{\text{Band4}}}$
TVI[82]	Transformed vegetation index	$\sqrt{\text{NDVI}+0.5}$
VARI700[83]	Visible atmospherically resistant index 700	$\frac{\text{Band5}-1.7*\text{Band4}+0.7*\text{Band2}}{\text{Band5}+2.3*\text{Band4}-1.3*\text{Band2}}$
VARIgreen[83]	Visible atmospherically resistant index green	$\frac{\text{Band3}-\text{Band4}}{\text{Band3}+\text{Band4}-\text{Band2}}$
VI700[84]	Vegetation index 700	$\frac{\text{Band5}-\text{Band4}}{\text{Band5}+\text{Band4}}$
WDRVI[85]	Wide dynamic range vegetation index	$\frac{0.1*\text{Band8}-\text{Band4}}{0.1*\text{Band8}+\text{Band4}}$

Table 2 Crop type and number of fields.

Crop type	Training data	Validation data	Test data
Beans	1132	566	567
Beetroot	774	387	387
Grassland	1055	527	528
Maize	500	250	250
Potato	1226	613	613
Wheat	1632	816	816

overfit. If it is too small, there may be underfitting. It controls the trade-off between errors of the SVM on training data and margin maximization ($C = \infty$ leads to hard margin SVM). The γ value defines how far the influence of a single training example reaches, with low values meaning "far" and high values meaning "close."

RF is an ensemble learning technique composed of multiple decision trees based on random bootstrapped samples of the training data.[88] The output is determined by a majority vote of the results of decision trees. There are two user-defined hyperparameters including the number of trees ($n$tree) and the number of variables used to split the nodes ($m$try). If $n$tree is made larger, the generalization error always converges, and over-training will not be a problem. On the other hand, a reduction in $m$try makes each individual decision tree weaker.

The best combinations of these hyperparameters were determined using the Gaussian process, Bayesian optimization,[89] which has been widely applied for hyperparameter tuning of machine learning algorithms.[1]

Ensemble machine learning methods have been used to obtain better predictive performance than from single learning algorithms, and the SL methodology has been proposed.[90] In this method, given algorithms are combined through a convex weighted combination to minimize cross-validated errors. First, classification models based on RF or SVM were trained as the base algorithms using the training data. Next, a 10-fold cross validation was performed on each and the cross-validated predicted results were obtained. N is the number of rows in the training data, cross-validated predicted results were combined, and an N by two matrices was obtained as the "level-one" data and meta-learning model was generated. To predict the test data, the predictions from the base learners were fed into the metalearning model to generate the ensemble prediction. The data-based sensitivity analysis (DSA),[91] which performs a pure black box use of the fitted models by querying the fitted models with sensitivity samples and recording their responses, was applied for assessing the sensitivity of the classification models.

2.4 *Accuracy Assessment*

Classification accuracies were evaluated based on the simple measures of quantity disagreement (QD) and allocation disagreement (AD).[92] They provide an effective summary of confusion matrices.[93]

The proportion of fields that are classified as crop i and their actual classes are crop j (P_{ij}) is expressed in the following

$$P_{ij} = W_i \frac{n_{ij}}{n_{i+}}, \tag{1}$$

where W_i is the fields classified as crop i, n_{ij} is the number of fields classified as crop i, and their actual classes are crop j. n_{i+} is the row totals of the confusion matrix. In this case, AD and QD are calculated using the following:

$$\mathrm{AD}_i = 2\ \min(p_{i+}, p_{+i}) - 2p_{ii}, \tag{2}$$

$$\mathrm{AD} = \frac{1}{2}\sum_{i=1}^{N_c} AD_i, \tag{3}$$

$$\mathrm{QD}_i = |p_{i+} - p_{+i}|, \tag{4}$$

$$\mathrm{QD} = \frac{1}{2}\sum_{i=1}^{N_c} \mathrm{QD}_i, \tag{5}$$

where N_c is the number of classes (six in this study), p_{i+} and p_{+i} are the row and column totals of the confusion matrix, AD_i is the allocation disagreement of crop i, and QD_i is the quantity disagreement of crop i, respectively. The sum of QD_i (QD) and AD_i (AD) are calculated and the total disagreement can be evaluated by the sum of QD and AD.[92]

In addition, three indicators including overall accuracy [OA, Eq. (6)], producer's accuracy [PA, Eq. (7)], and user's accuracy [UA, Eq. (8)] were calculated because they have widely been applied for assessing classification accuracies

$$\mathrm{OA} = \sum_{i=1}^{N} p_{ii}/N, \tag{6}$$

$$\mathrm{PA} = p_{ii}/R_i, \tag{7}$$

$$\mathrm{UA} = p_{ii}/C_i, \tag{8}$$

where N is the number of fields, R_i and C_i represent the total number of crop i in the correct data and the total number from the classification results, respectively. McNemar's test[94] has been used to judge whether the differences between two given classification results were significant,[95] and it was also applied in this study.

3 Results and Discussion

3.1 *Classification Accuracy*

Crop classification maps are shown in Fig. 2, the maximum, minimum, and averaged accuracies of 10 repetitions and confusion matrices when all the repetitions were merged are shown in Tables 3 and 4. Averaged OAs were 89.0% for RF, 90.6% for SVM, and 91.6% for the ensemble machine learning method and the mean PAs and mean UAs derived using the machine learning algorithms were >0.8, excepting those of RF (mean UA for maize was 0.797). All machine learning algorithms performed well in classifying croplands. Especially, the good accuracies were confirmed for the PAs and UAs for wheat (>93.8%) and beet (>89.9%). However, the chi-square values based on McNemar's tests were 12.02 to 40.60, 27.78 to 62.43, and 17.00 to 51.60 for R—SVM, RF—SL, and SVM—SL, respectively. As a result, significant differences were confirmed among the results of three machine learning algorithms ($p < 0.05$).

Classification results by SL had the best OA and AD + QD (8.5%) and SVM had a slightly better PA of wheat (97.1%). On the contrary, identifying maize fields was difficult due to the similarity in their reflectance. Grasses cultivation employs fewer controls and then a lot of weeds were mixed with timothy and orchard grass in grasslands. As a result, variation in reflectance features was larger than in other crop types, causing misclassifications of relatively large fields.

Figure 3 shows the relationship between field area and misclassified fields for each algorithm after 10 repetitions (i.e., the total number is 10 times of that of the test data). More than 75% of the misclassified fields were <200 a in area for all algorithms, and 95.1% (RF), 95.5% (SVM), and 96.1% (SL) of misclassified fields were below 450 a. Applying stacking made the model more robust for classifying smaller fields and the number of misclassified croplands decreased

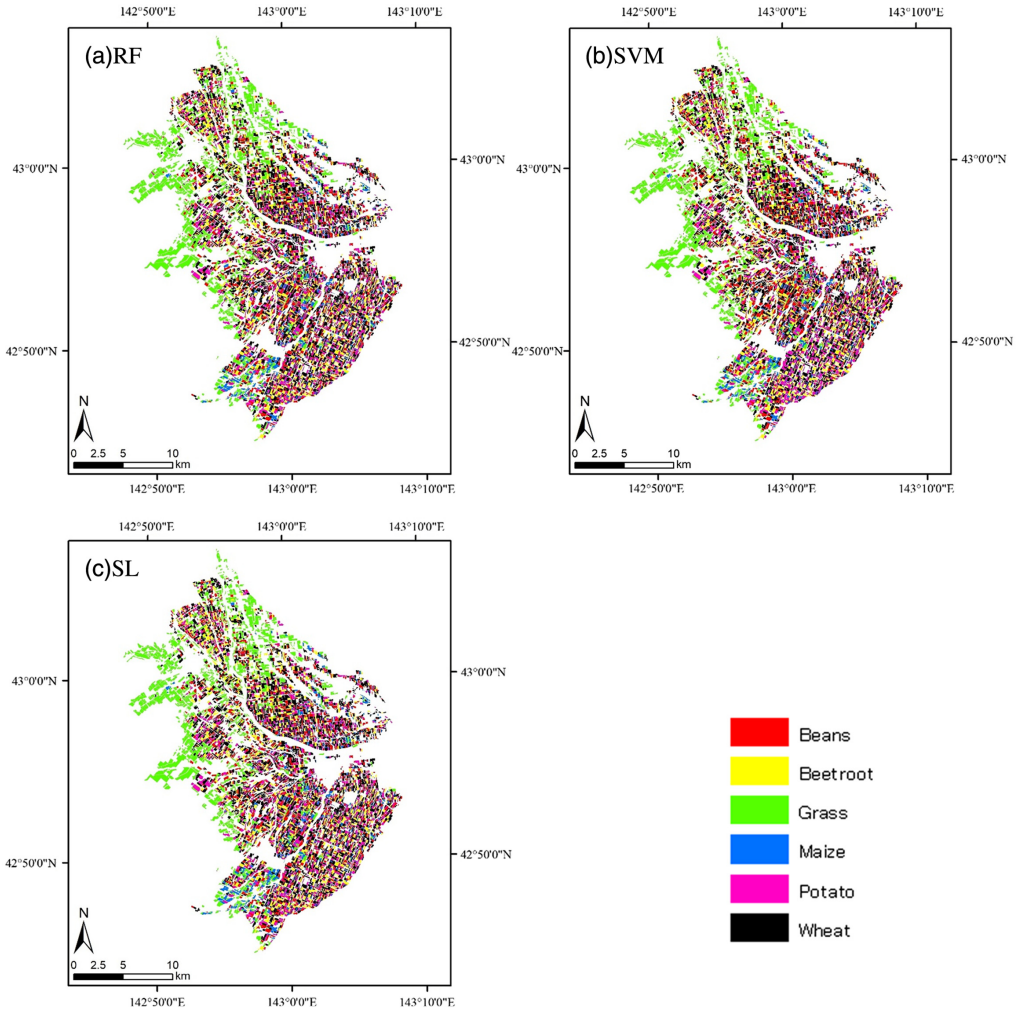

Fig. 2 Crop classification map generated by (a) RF, (b) SVM, and (c) SL.

(813 fields for smaller than 50 a) compared with the results by RF (909 fields for smaller than 50 a) and SVM (855 fields for smaller than 50 a). It was especially useful for identifying beans fields. It was not effective for identifying small grasslands as grass cultivation employs fewer controls and many weeds were present in grasslands. However, stacking was useful for identifying grasslands more than 500 a, which had a certain homogeneity with *Dactylis glomerata* or *Phleum pretense* in the MSI image.

3.2 *Sensitive Factor Analysis*

Reflectance values obtained from Sentinel-2A are shown in Fig. 4. Differences in reflectance were particularly clear between wheat and beans as the wheat harvest was finished on 11 August and the reflectance of wheat fields was similar to that of bare soil. Beetroot had the steepest gradient between bands 5 and 6 and some differences in the reflectance values at band 11 were confirmed between maize and potato. Differences in the reflectance patterns between grass and beans were not clear.

To clarify which variables contributed to identifying each crop type, DSA was conducted for each algorithm and their importance values were calculated.

For identifying beans fields, Datt3 (6.0%, 6.6%, and 6.3% for RF, SVM, and SL, respectively) and REIP (6.4%, 8.2%, and 7.3% for RF, SVM, and SL, respectively) played important roles in the three algorithms. Some variables (the reflectance values at bands 2 and 3, AFRI2.1, CVI and NDSI) possessed importance values of >5.0% in the RF-based model, whereas no

Table 3 Classification accuracies of each algorithm.

	RF			SVM			SL		
	Minimum (%)	Maximum (%)	Mean ± std (%)	Minimum (%)	Maximum (%)	Mean ± std (%)	Minimum (%)	Maximum (%)	Mean ± std (%)
PA									
Beans	80.6	86.4	83.4 ± 1.6	81.1	90.5	86.2 ± 2.2	84.7	90.3	87.6 ± 1.4
Beet	89.9	94.8	93.0 ± 1.3	91.0	96.4	94.5 ± 1.5	93.8	96.1	95.1 ± 0.6
Grassland	84.3	88.3	86.0 ± 1.2	86.7	93.8	89.4 ± 2.5	89.8	94.3	92.1 ± 1.4
Maize	78.8	84.8	80.8 ± 1.7	78.8	87.6	83.0 ± 3.1	81.2	87.6	84.6 ± 1.8
Potato	82.9	89.7	87.0 ± 1.8	83.5	89.9	87.6 ± 1.9	84.0	89.7	88.1 ± 1.6
Wheat	96.4	97.9	97.0 ± 0.5	96.3	97.5	97.1 ± 0.4	95.7	97.5	97.0 ± 0.7
UA									
Beans	84.9	88.6	86.8 ± 1.1	82.0	91.4	86.4 ± 2.9	83.4	90.3	88.6 ± 2.0
Beet	94.5	96.9	95.6 ± 0.8	94.3	97.3	95.7 ± 0.9	95.1	97.1	96.0 ± 0.6
Grassland	88.0	93.3	91.0 ± 1.4	89.9	96.6	94.0 ± 2.3	93.8	97.7	95.7 ± 1.1
Maize	77.8	82.0	79.7 ± 1.3	78.4	87.3	81.9 ± 2.2	81.4	85.2	83.6 ± 1.4
Potato	78.5	83.1	81.5 ± 1.2	82.1	87.8	85.2 ± 1.9	83.0	86.8	85.4 ± 1.1
Wheat	93.8	96.1	95.0 ± 0.7	94.5	97.2	95.9 ± 0.8	95.1	97.2	96.2 ± 0.6
OA	88.5	89.4	89.0 ± 0.2	89.3	92.0	90.6 ± 0.9	90.2	92.2	91.6 ± 0.6
κ	85.9	87.0	86.5 ± 0.3	86.8	90.2	88.4 ± 1.1	88.0	90.5	89.6 ± 0.8
AD	8.0	9.9	9.0 ± 0.6	6.5	9.7	7.9 ± 1.0	6.5	8.8	7.3 ± 0.7
QD	1.3	2.8	2.0 ± 0.5	0.7	2.5	1.5 ± 0.6	0.6	2.3	1.2 ± 0.5

variables except for Datt3 and REIP had importance values of >5.0% for SVM and SL. Even though the importance values of GEMI, Maccioni, and MNSI in SVM were <5.0%, they were more than five times those in RF. AFRI1.6 and SIWSI were useful for identifying beetroot fields and AFRI1.6 occupied 11.1%, 6.8%, and 9.0% and SIWSI occupied 10.6%, 7.1%, and 8.9% of the importance for RF, SVM, and SL, respectively. GEMI and NDSI also had importance values of >10% for RF, but were <5% for the others. In contrast, REIP was useful in SVM and it occupied 9.1% of the importance in SVM. AFRI1.6, REIP, and MNSI were effective for identifying grassland for all algorithms, whereas SIWSI played an important role (7.8%) for RF and the reflectance at band 6 played an important role (8.2%) for SVM. For identifying maize fields, no variable had importance values >5.0% for any algorithm, but the importance value of REIP was 25.3% for SVM (2.9% for RF). CRI550, CRI700, and MSBI were 9.1%, 12.9%, and 5.6% in RF, respectively (those in SVM were 2.4%, 2.2%, and 3.6%, respectively). REIP played the greatest role for identifying potato fields in all algorithms (12.8%, 6.9% and 9.9% for RF, SVM, and SL, respectively). The importance values of CCCI and CVI were also high in RF (9.9%) but those in SVM were <3.0%. In contrast, Maccioni had an importance of 6.9% in SVM but in RF was 1.4%. REIP also played a great role for identifying wheat fields in SVM, but 1.2% of the importance value was confirmed in RF while AVI occupied 15.1% in RF (1.2% in SVM). However, the original reflectance values possessed importance values of <1.0%.

In this season, the photosynthetic activities of each crop type were different; maize is a C4 plant, beans and beetroot were in their growing season, grassland was after second harvest, potato growth was inhibited by chemicals for easy harvesting, and wheat fields were cultivated.

Table 4 Confusion matrices for (a) RF, (b) SVM, and (c) SL.

		Reference data					
		Beans	Beetroot	Grasslands	Maize	Potato	Wheat
		(a) RF					
Classified data	Beans	4726	59	247	100	287	26
	Beet	48	3599	23	28	65	1
	Grasslands	172	65	4543	52	116	43
	Maize	139	21	128	2019	177	48
	Potato	503	119	230	235	5332	123
	Wheat	82	7	109	66	153	7919
		(b) SVM					
Classified data	Beans	4888	77	212	119	333	34
	Beet	61	3659	17	22	63	2
	Grasslands	110	34	4720	40	70	49
	Maize	112	14	130	2076	166	40
	Potato	429	79	121	189	5368	115
	Wheat	70	7	80	54	130	7920
		(c) SL					
Classified data	Beans	4965	82	105	83	333	42
	Beet	61	3680	11	17	61	3
	Grasslands	59	17	4861	37	52	53
	Maize	85	8	121	2114	169	32
	Potato	426	77	113	200	5403	112
	Wheat	74	6	69	49	112	7918

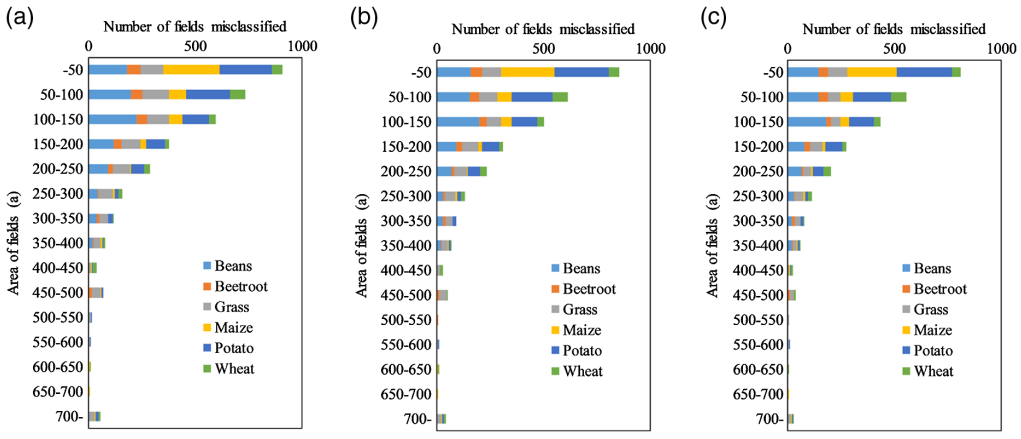

Fig. 3 Relationship between field area and misclassified fields (a) RF, (b) SVM, and (c) SL.

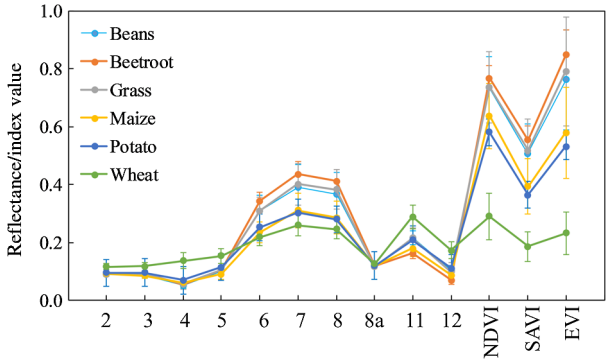

Fig. 4 Mean reflectance spectra and standard deviations of each crop.

In addition to indices related to chlorophyll content, the additional use of shortwave infrared data contributed to the estimation of photosynthetic pigments, water, nitrogen, cellulose, lignin, phenols, and leaf mass per area (e.g., NDSI). As a result, vegetation indices had greater influence on the classification results than the original reflectance. However, there were differences among algorithms in which vegetation indices were more important. The importance values in SL were near the averaged values of RF and SVM. So, the differences in importance between RF and SVM were useful when stacking was applied, and the modification contributed to identifying croplands with higher accuracies.

4 Conclusions and Future Work

Cropland classifications were conducted using a single image from Sentinel-2 MSI and the suitability and accuracy of vegetation indices from the original reflectance data from Sentinel-2 MSI were assessed.

Of the two algorithms applied (RF and SVM), the accuracy of SVM was superior and 89.3% to 92.0% of OAs were confirmed. Furthermore, stacking contributed to higher OAs (90.2% to 92.2%) and significant differences were confirmed with the results of SVM. Based on DSA, the vegetation indices calculated from the original reflectance from Sentinel-2 MSI data were useful to identify the specific crop types. Although the vegetation indices that played the largest roles were different between RF and SVM, stacking helped to modify and reduce the importance of specific variables, which might prevent overfitting. Stacking should be utilized to monitor agricultural fields for improving classification accuracies.

The field is used as a basic unit in classification and some problems related to the borders of fields remain to be resolved. We are planning to evaluate the potential of geographic object-based image analysis in conjunction with MSI data and address this question in future work.

Disclosures

No potential conflicts of interest are reported by the authors.

Acknowledgments

The authors would like to thank Tokachi Nosai for providing the field data.

References

1. R. Sonobe et al., "Assessing the suitability of data from Sentinel-1A and 2A for crop classification," *GISci. Remote Sens.* **54**, 918–938 (2017).
2. R. Sonobe et al., "Estimating leaf carotenoid contents of shade grown tea using hyperspectral indices and PROSPECT-D inversion," *Int. J. Remote Sens.* **39**, 1306–1320 (2018).
3. C. Rankine et al., "Comparing MODIS and near-surface vegetation indexes for monitoring tropical dry forest phenology along a successional gradient using optical phenology towers," *Environ. Res. Lett.* **12**, 105007 (2017).

4. S. S. Liu et al., "Regional-scale winter wheat phenology monitoring using multisensor spatio-temporal fusion in a South Central China growing area," *J. Appl. Remote Sens.* **10**, 046029 (2016).
5. J. Vithanage, S. N. Miller, and K. Driese, "Land cover characterization for a watershed in Kenya using MODIS data and Fourier algorithms," *J. Appl. Remote Sens.* **10**, 045015 (2016).
6. R. Sonobe et al., "Evaluating metrics derived from Landsat 8 OLI imagery to map crop cover," *Geocarto Int.* (2018).
7. G. P. Asner, "Biophysical and biochemical sources of variability in canopy reflectance," *Remote Sens. Environ.* **64**, 234–253 (1998).
8. M. A. Pena, R. Liao, and A. Brenning, "Using spectrotemporal indices to improve the fruit-tree crop classification accuracy," *ISPRS J. Photogramm. Remote Sens.* **128**, 158–169 (2017).
9. D. Bankestad and T. Wik, "Growth tracking of basil by proximal remote sensing of chlorophyll fluorescence in growth chamber and greenhouse environments," *Comput. Electron. Agric.* **128**, 77–86 (2016).
10. Z. Wang et al., "Spatiotemporal variations of forest phenology in the Qinling Mountains and its response to a critical temperature of 10 degrees C," *J. Appl. Remote Sens.* **12**, 022202 (2018).
11. M. Morin et al., "Agreement analysis and spatial sensitivity of multispectral and hyperspectral sensors in detecting vegetation stress at management scales," *J. Appl. Remote Sens.* **11**, 046025 (2017).
12. C. J. Tucker, "Red and photographic infrared linear combinations for monitoring vegetation," *Remote Sens. Environ.* **8**, 127–150 (1979).
13. A. R. Huete, "A soil-adjusted vegetation index (SAVI)," *Remote Sens. Environ.* **25**, 295–309 (1988).
14. A. Huete et al., "Overview of the radiometric and biophysical performance of the MODIS vegetation indices," *Remote Sens. Environ.* **83**, 195–213 (2002).
15. C. E. Holden and C. E. Woodcock, "An analysis of Landsat 7 and Landsat 8 underflight data and the implications for time series investigations," *Remote Sens. Environ.* **185**, 16–36 (2016).
16. M. Belgiu and O. Csillik, "Sentinel-2 cropland mapping using pixel-based and object-based time-weighted dynamic time warping analysis," *Remote Sens. Environ.* **204**, 509–523 (2018).
17. M. Immitzer, F. Vuolo, and C. Atzberger, "First experience with Sentinel-2 data for crop and tree species classifications in Central Europe," *Remote Sens.* **8**, 166 (2016).
18. Y. Palchowdhuri et al., "Classification of multi-temporal spectral indices for crop type mapping: a case study in Coalville, UK," *J. Agric. Sci.* **156**, 24–36 (2018).
19. A. Novelli et al., "Performance evaluation of object based greenhouse detection from Sentinel-2 MSI and Landsat 8 OLI data: a case study from Almeria (Spain)," *Int. J. Appl. Earth Obs. Geoinf.* **52**, 403–411 (2016).
20. Y. Du et al., "Water Bodies' mapping from Sentinel-2 imagery with modified normalized difference water index at 10-m spatial resolution produced by sharpening the SWIR Band," *Remote Sens.* **8**, 354 (2016).
21. G. Biau and E. Scornet, "A random forest guided tour," *Test* **25**, 197–227 (2016).
22. S. Ferrant et al., "Detection of irrigated crops from Sentinel-1 and Sentinel-2 data to estimate seasonal groundwater use in South India," *Remote Sens.* **9**, 1119 (2017).
23. A. O. Onojeghuo et al., "Mapping paddy rice fields by applying machine learning algorithms to multi-temporal Sentinel-1A and Landsat data," *Int. J. Remote Sens.* **39**, 1042–1067 (2018).
24. R. Sonobe et al., "Discrimination of crop types with TerraSAR-X-derived information," *Phys. Chem. Earth. Parts A, B, C* **83–84**, 2–13 (2015).
25. J. K. Gilbertson and A. van Niekerk, "Value of dimensionality reduction for crop differentiation with multi-temporal imagery and machine learning," *Comput. Electron. Agric.* **142**, 50–58 (2017).

26. R. Sonobe et al., "Random forest classification of crop type using multi- temporal TerraSAR- X dual- polarimetric data," *Remote Sens. Lett.* **5**, 157–164 (2014).
27. G. Camps-Valls et al., "Robust support vector method for hyperspectral data classification and knowledge discovery," *IEEE Trans. Geosci. Remote Sens.* **42**, 1530–1542 (2004).
28. M. Drusch et al., "Sentinel-2: ESA's optical high-resolution mission for GMES operational services," *Remote Sens. Environ.* **120**, 25–36 (2012).
29. U.S. Geological Survey, "EarthExplorer," https://earthexplorer.usgs.gov/ (14 December 2016).
30. A. Chatziantoniou, G. P. Petropoulos, and E. Psomiadis, "Co-orbital Sentinel 1 and 2 for LULC mapping with emphasis on Wetlands in a Mediterranean setting based on machine learning," *Remote Sens.* **9**, 1259 (2017).
31. E. M. D. Silveira et al., "Assessment of geostatistical features for object-based image classification of contrasted landscape vegetation cover," *J. Appl. Remote Sens.* **11**, 036004 (2017).
32. A. Karnieli et al., "AFRI—aerosol free vegetation index," *Remote Sens. Environ.* **77**, 10–21 (2001).
33. A. A. Gitelson, O. B. Chivkunova, and M. N. Merzlyak, "Nondestructive estimation of anthocyanins and chlorophylls in anthocyanic leaves," *Am. J. Bot.* **96**, 1861–1868 (2009).
34. Y. J. Kaufman and D. Tanre, "Atmospherically resistant vegetation index (ARVI) for EOS-MODIS," *IEEE Trans. Geosci. Remote Sens.* **30**, 261–270 (1992).
35. F. Baret and G. Guyot, "Potentials and limits of vegetation indices for LAI and APAR assessment," *Remote Sens. Environ.* **35**, 161–173 (1991).
36. P. Ashburn, "The vegetative index number and crop identification," in *The LACIE Symp. Proc. of the Technical Session*, pp. 843–855 (1978).
37. C. G. Yang, J. H. Everitt, and J. M. Bradford, "Airborne hyperspectral imagery and linear spectral unmixing for mapping variation in crop yield," *Precis. Agric.* **8**, 279–296 (2007).
38. O. B. Chivkunova et al., "Reflectance spectral features and detection of superficial scald -induced browning in storing apple fruit," *J. Russ. Phytopathol. Soc.* **2**, 73–77 (2001).
39. D. W. Hancock and C. T. Dougherty, "Relationships between blue- and red-based vegetation indices and leaf area and yield of alfalfa," *Crop Sci.* **47**, 2547–2556 (2007).
40. M. S. Kim et al., "The use of high spectral resolution bands for estimating absorbed photo-synthetically active radiation (A par)," in *The 6th Int. Symp. on Physical Measurements and Signatures in Remote Sensing*, Val D'Isere, France (1994).
41. D. M. El-Shikha et al., "Remote sensing of cotton nitrogen status using the Canopy Chlorophyll Content Index (CCCI)," *Trans. ASABE* **51**, 73–82 (2008).
42. A. A. Gitelson, M. N. Merzlyak, and O. B. Chivkunova, "Optical properties and non-destructive estimation of anthocyanin content in plant leaves," *Photochem. Photobiol.* **74**, 38–45 (2001).
43. E. R. Hunt et al., "Remote sensing leaf chlorophyll content using a visible band index," *Agron. J.* **103**, 1090–1099 (2011).
44. B. Datt, "Remote sensing of water content in eucalyptus leaves," *Aust. J. Bot.* **47**, 909–923 (1999).
45. B. Datt, "Remote sensing of chlorophyll a, chlorophyll b, chlorophyll a+b, and total carotenoid content in eucalyptus leaves," *Remote Sens. Environ.* **66**, 111–121 (1998).
46. A. J. Richardson and C. L. Wiegand, "Distinguishing vegetation from soil background information," *Photogramm. Eng. Remote Sens.* **43**, 1541–1552 (1977).
47. T. Miura et al., "Inter-comparison of ASTER and MODIS surface reflectance and vegetation index products for synergistic applications to natural resource monitoring," *Sensors* **8**, 2480–2499 (2008).
48. Z. Y. Jiang et al., "Development of a two-band enhanced vegetation index without a blue band," *Remote Sens. Environ.* **112**, 3833–3845 (2008).
49. A. A. Gitelson, Y. J. Kaufman, and M. N. Merzlyak, "Use of a green channel in remote sensing of global vegetation from EOS-MODIS," *Remote Sens. Environ.* **58**, 289–298 (1996).

50. F. M. Wang, J. F. Huang, and L. Chen, "Development of a vegetation index for estimation of leaf area index based on simulation modeling," *J. Plant Nutr.* **33**, 328–338 (2010).
51. C. J. Tucker, "Monitoring corn and soybean crop development with hand-held radiometer spectral data," *Remote Sens. Environ.* **8**, 237–248 (1979).
52. B. Pinty and M. M. Verstraete, "GEMI: a non-linear index to monitor global vegetation from satellites," *Vegetatio* **101**, 15–20 (1992).
53. N. Gobron et al., "Advanced vegetation indices optimized for up-coming sensors: design, performance, and applications," *IEEE Trans. Geosci. Remote Sens.* **38**, 2489–2505 (2000).
54. G. Rondeaux, M. Steven, and F. Baret, "Optimization of soil-adjusted vegetation indices," *Remote Sens. Environ.* **55**, 95–107 (1996).
55. F.-M. Wang et al., "New vegetation index and its application in estimating leaf area index of rice," *Rice Sci.* **14**, 195–203 (2007).
56. E. P. Glenn, P. L. Nagler, and A. R. Huete, "Vegetation index methods for estimating evapotranspiration by remote sensing," *Surv. Geophys.* **31**, 531–555 (2010).
57. R. Escadafal, A. Belghith, and H. Ben-Moussa, "Indices spectraux pour la degradation des milieux naturels en Tunisie aride," in *6e Symp. Int. sur les mesures physiques et signatures en teledetection*, Val d'Isere, France, pp. 253–259 (1994)
58. R. E. Crippen, "Calculating the vegetation index faster," *Remote Sens. Environ.* **34**, 71–73 (1990).
59. A. Maccioni, G. Agati, and P. Mazzinghi, "New vegetation indices for remote measurement of chlorophylls based on leaf directional reflectance spectra," *J. Photochem. Photobiol. B* **61**, 52–61 (2001).
60. C. S. T. Daughtry et al., "Estimating corn leaf chlorophyll concentration from leaf and canopy reflectance," *Remote Sens. Environ.* **74**, 229–239 (2000).
61. J. U. H. Eitel et al., "Using in-situ measurements to evaluate the new RapidEye (TM) satellite series for prediction of wheat nitrogen status," *Int. J. Remote Sens.* **28**, 4183–4190 (2007).
62. D. Haboudane et al., "Hyperspectral vegetation indices and novel algorithms for predicting green LAI of crop canopies: modeling and validation in the context of precision agriculture," *Remote Sens. Environ.* **90**, 337–352 (2004).
63. P. N. Misra, S. G. Wheeler, and R. E. Oliver, "Kauth-Thomas brigthness and greenness axes," Contract NASA 9-14350, pp. 23–46 (1977).
64. R. Main et al., "An investigation into robust spectral indices for leaf chlorophyll estimation," *ISPRS J. Photogramm. Remote Sens.* **66**, 751–761 (2011).
65. J. Qi et al., "A modified soil adjusted vegetation index," *Remote Sens. Environ.* **48**, 119–126 (1994).
66. J. M. Chen, "Evaluation of vegetation indices and a modified simple ratio for boreal applications," *Can. J. Remote Sens.* **22**, 229–242 (1996).
67. J. M. Chen and J. Cihlar, "Retrieving leaf area index of boreal conifer forests using Landsat TM images," *Remote Sens. Environ.* **55**, 153–162 (1996).
68. C. Key and N. Benson, Landscape assessment: ground measure of severity; the composite burn index, and remote sensing of severity, the normalized burn index and remote sensing of severity, the normalized burn ratio, in *FIREMON: Fire Effects Monitoring and Inventory System*, D. Lutes et al., Eds., pp. 1–51, Rocky Mountains Research Station, USDA Forest Service, Fort Collins, Colorado (2005).
69. P. J. Zarco-Tejada et al., "Scaling-up and model inversion methods with narrowband optical indices for chlorophyll content estimation in closed forest canopies with hyperspectral data," *IEEE Trans. Geosci. Remote Sens.* **39**, 1491–1507 (2001).
70. M. A. Hardisky, V. Klemas, and R. M. Smart, "The influences of soil salinity, growth form, and leaf moisture on the spectral reflectance of Spartina Alterniflora canopies," *Photogramm. Eng. Remote Sens.* **49**, 77–84 (1983).
71. E. M. Barnes et al., "Coincident detection of crop water stress, nitrogen status and canopy density using ground based multispectral data," in *Proc. of Fifth Int. Conf. on Precision Agriculture and Other Resource Management ASA-CSSA-SSSA*, Madison, USA (2000).

72. A. Dehni and M. Lounis, "Remote sensing tetchniques for salt affected soil mapping: application to the Oran Region of Algeria," *Procedia Eng.* **33**, 188–198 (2012).
73. D. Haboudane et al., "Integrated narrow-band vegetation indices for prediction of crop chlorophyll content for application to precision agriculture," *Remote Sens. Environ.* **81**, 416–426 (2002).
74. G. Metternicht, "Vegetation indices derived from high-resolution airborne videography for precision crop management," *Int. J. Remote Sens.* **24**, 2855–2877 (2003).
75. N. H. Broge and E. Leblanc, "Comparing prediction power and stability of broadband and hyperspectral vegetation indices for estimation of green leaf area index and canopy chlorophyll density," *Remote Sens. Environ.* **76**, 156–172 (2001).
76. I. Herrmann et al., "LAI assessment of wheat and potato crops by VEN mu S and Sentinel-2 bands," *Remote Sens. Environ.* **115**, 2141–2151 (2011).
77. J. Clevers et al., "Derivation of the red edge index using the MERIS standard band setting," *Int. J. Remote Sens.* **23**, 3169–3184 (2002).
78. J. Penuelas, F. Baret, and I. Filella, "Semi-empirical indices to assess Carotenoids/Chlorophyll-a ratio from leaf spectral reflectance," *Photosynthetica* **31**, 221–230 (1995).
79. R. Fensholt and I. Sandholt, "Derivation of a shortwave infrared water stress index from MODIS near- and shortwave infrared data in a semiarid environment," *Remote Sens. Environ.* **87**, 111–121 (2003).
80. L. Lymburner, P. J. Beggs, and C. R. Jacobson, "Estimation of canopy-average surface-specific leaf area using Landsat TM data," *Photogramm. Eng. Remote Sens.* **66**, 183–191 (2000).
81. D. Haboudane et al., "Remote estimation of crop chlorophyll content using spectral indices derived from hyperspectral data," *IEEE Trans. Geosci. Remote Sens.* **46**, 423–437 (2008).
82. J. W. Rouse et al., "Monitoring vegetation systems in the great plains with ERTS," in *Third Earth Resources Technology Satellite-1 Symp.*, S. C. Freden, E. P. Mercanti, and M. A. Becker, Eds., pp. 309–317, NASA, Washington, D.C (1974).
83. A. A. Gitelson et al., "Non-destructive and remote sensing techniques for estimation of vegetation status," in *Third European Conf. on Precision Agriculture*, Montpellier, France, pp. 301–306 (2001).
84. A. A. Gitelson et al., "Novel algorithms for remote estimation of vegetation fraction," *Remote Sens. Environ.* **80**, 76–87 (2002).
85. A. A. Gitelson, "Wide dynamic range vegetation index for remote quantification of biophysical characteristics of vegetation," *J. Plant Physiol.* **161**, 165–173 (2004).
86. T. Hastie, R. Tibshirani, and J. Friedman, *The Elements of Statistical Learning: Data Mining, Inference, and Prediction*, 2nd ed., Springer-Verlag, New York (2009)
87. C. Cortes and V. Vapnik, "Support-vector networks," *Mach. Learn.* **20**, 273–297 (1995).
88. L. Breiman, "Random forests," *Mach. Learn.* **45**, 5–32 (2001).
89. J. Bergstra and Y. Bengio, "Random search for hyper-parameter optimization," *J. Mach. Learn. Res.* **13**, 281–305 (2012).
90. M. J. van der Laan, E. C. Polley, and A. E. Hubbard, "Super learner," *Stat. Appl. Genet. Mol. Biol.* **6**, 1–23 (2007).
91. P. Cortez and M. J. Embrechts, "Using sensitivity analysis and visualization techniques to open black box data mining models," *Inf. Sci.* **225**, 1–17 (2013).
92. R. Pontius and M. Millones, "Death to Kappa: birth of quantity disagreement and allocation disagreement for accuracy assessment," *Int. J. Remote Sens.* **32**, 4407–4429 (2011).
93. M. Story and R. Congalton, "Accuracy assessment: a user's perspective," *Photogramm. Eng. Remote Sens.* **52**, 397–399 (1986).
94. Q. McNemar, "Note on the sampling error of the difference between correlated proportions or percentages," *Psychometrika* **12**, 153–157 (1947).
95. G. M. Foody, "Thematic map comparison: evaluating the statistical significance of differences in classification accuracy," *Photogramm. Eng. Remote Sens.* **70**, 627–633 (2004).

Biographies for the authors are not available.